Pergamon

Cement and Concrete Research 30 (2000) 1723–1730

CEMENT AND CONCRETE RESEARCH

Equivalent circuit model for AC electrochemical impedance spectroscopy of concrete

Guangling Song*

Department of Mining, Minerals and Materials Engineering, The University of Queensland, St. Lucia, Brisbane, QLD 4072, Australia

Received 16 March 1999; accepted 7 August 2000

Abstract

An equivalent circuit model for AC electrochemical impedance spectroscopy (EIS) of concrete has been proposed, which contains parameters R_{CCP}, the resistance of the continuously connected micro-pores in the concrete; R_{CP}, the resistance of the discontinuously connected micro-pores, blocked by cement paste layers in the concrete; C_{mat}, the capacitance across the concrete matrix; and C_{DP}, the capacitance of the cement paste layers blocking the discontinuously connected micro-pores in the concrete. The proposed model can successfully explain the experimental phenomena observed by other researchers, such as the emergence of the capacitive loops in high-frequency range, the influences of hydration time, silica fume, water/cement ratio on the loops, etc. © 2000 Elsevier Science Ltd. All rights reserved.

Keywords: Concrete; Cement; Model; Microstructure; Electrochemical impedance spectroscopy (EIS)

1. Introduction

Microstructure of concrete is of considerable importance because it governs the mechanical properties and durability of the concrete, and has significant influences on corrosion performance of the reinforcing steel in the concrete.

In the past decade, AC electrochemical impedance spectroscopy (EIS), one of the non-destructive methods, has been demonstrated to be a promising technique for its capability of revealing the microstructure of concrete in high-frequency region, above kilohertz [1–8]. The high-frequency EIS spectra in the Nyquist diagram are usually found to be a capacitive loop, which is generally attributed to the resistance of concrete bulk and the dispersive capacitance of micro-pore network in the concrete. In most cases, such a capacitive loop has been simulated with a simple equivalent circuit composed of a resistance R_1 and a capacitance C_1 connected together in parallel [4–16].

In some studies [6,8,15–18], it has been found that the measured impedance (Z) of a cement paste does not tend towards the origin of the Nyquist diagram along the high-frequency capacitive loop as frequency increases; instead, it intersects the Z_r axis at a distance of R_0 from the origin. In this case, the equivalent circuit for concrete should actually be a R_1 and a C_1 in parallel, then connecting to a resistance R_0 in series.

Different interpretations have been given to the measured R_0 in the high-frequency region. For example, Christensen et al. [17,18] defined R_0 as an offset resistance for curve fitting purpose, a meaningless parameter. Gu et al. [6–8] attributed R_0 mainly to the resistance of unhydrated cement and hydration products in their first model, and then to the resistance of the pore solution in their second model.

The above argument over the explanation for AC EIS spectra in the high-frequency region mainly originates from using improper AC EIS models of the microstructure of concrete. Even though several models [7,8,19–25] have been proposed by various researchers, most of them are not convincing in interpreting the EIS behaviours of cement paste, mortar, and concrete. For example, Whittington et al. [19] proposed a conduction model for concrete in 1981, which involved aggregate, cement paste, and aggregate/paste three conductive paths. Nevertheless, the model is impractical for the extremely low possibility of the aggregates in contact directly with each other (one by one) without thin cement paste layers at the contacting points. The multi-layer [7] and multi-cube [8] models apparently succeed in interpreting some EIS

* Tel.: +61-7-3365-4197; fax: +61-7-3365-3888.
E-mail address: g.song@minmet.uq.edu.au (G. Song).

PII: S0008-8846(00)00400-2

results. However, in some cases, unreasonable corollaries could result, such as the resistivity of concrete strongly dependent on the applied current or potential. Similarly, the "T" model [18] could account for the dielectric amplification behaviour of a cementitious system, but if it is employed to describe the EIS behaviour, in theory, current-dependent concrete resistivity would also be obtained. Compared with the "T" model, the barrer/pin-hole model by Ford et al. [25] has made some improvements on simulating the microstructure of a cementitious system, and can explain some EIS features. Unfortunately, some important factors, such as the porosity of cement paste, which could affect EIS features, have not been involved. Among those models, Macphee et al.'s [22–24] equivalent circuit could be most complicated, in which all the conductive paths of continuous pores, discontinuous pores, hydration products, unreacted cement, have been considered. Since the principal conductive paths in the model are mixed with those unimportant conductive paths, such as the unreacted cement, which has insignificant contribution to the current conduction, extracting resistance and capacitance values for individual microstructural features becomes extremely difficult [24]. Therefore, the model is impractical in application, and Cormack et al. [24] even stated that their early interpretation [23] of the EIS behaviours based on their model appeared to be incorrect.

In this paper, effort is made to establish a new equivalent circuit for concrete on the basic of the existing models, aimed at revealing the physical meanings of the parameters R_0, R_1, C_1, etc. obtained from EIS technique. It is hoped that the model is helpful to the understanding of concrete microstructure and properties, can offer more reasonable explanations for the EIS spectra obtained by other researchers, and will lead to a practical technique of extracting the meaningful parameters from the EIS results.

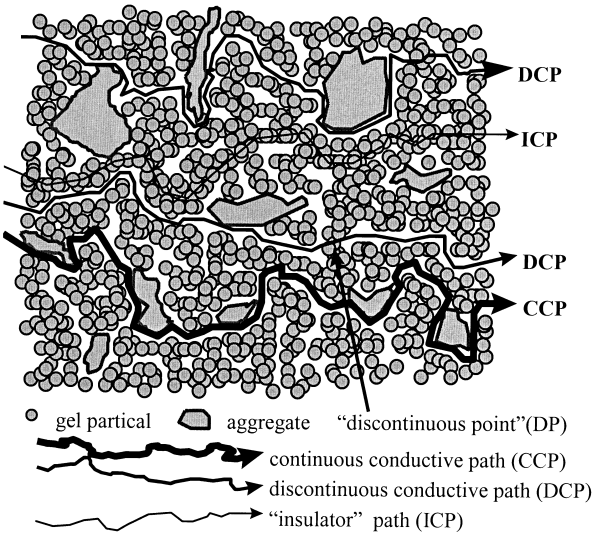

Fig. 1. Schematic representation of microstructure of concrete.

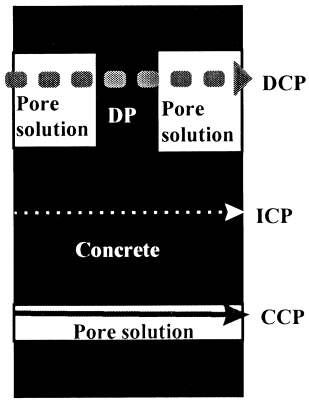

Fig. 2. Simplified microstructure of concrete.

2. Equivalent circuit model for concrete

In principle, the microstructure of concrete can be schematically illustrated as in Fig. 1. Basically, there are three kinds of paths in such a structure: (1) continuous conductive paths (CCPs), discontinuous conductive paths (DCPs), and "insulator" conductive paths (ICPs). The CCPs are the continuously connected micro-pores, which could be a series of capillary cavities connected through pore necks. The discontinuous micro-pores in the concrete form the DCPs, whose continuity is blocked by the cement paste layers, which is also denoted as "discontinuous points" (DPs) in this paper. The discontinuous pores can also be connected to continuous pores as dead ends. Apart from the DCPs and CCPs, the continuous concrete matrix, which is composed of cement paste particles, acts as "insulator" paths (ICPs) in the concrete.

Based on the above considerations, the microstructure of the concrete can be simplified into Fig. 2, in which the white areas represent pores and the black stands for cement paste mixed with aggregates. The porosity (φ) of the concrete can be represented by the ratio of the white areas over the whole block (white areas + black area) in Fig. 2.

The conductivity of the concrete depends on the impedance of all the three kinds of conductive paths, which can be incorporated into a circuit as shown in Fig. 3, and correspondingly, the total impedance (Z) of the concrete would be [Eq. (1)]:

$$Z = 1/(1/Z_{CCP} + 1/Z_{DCP} + 1/Z_{ICP}) \quad (1)$$

Theoretically, current conduction through CCP occurs by ions migrating in the pore solution, i.e., Ohm's law operates in this case. Therefore, the total impedance of all the CCPs

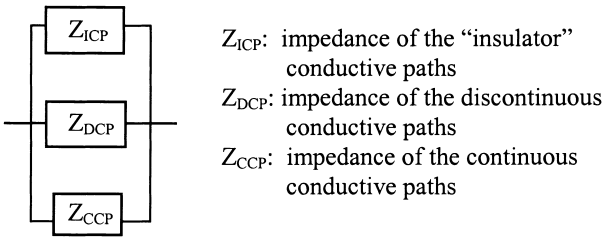

Fig. 3. Extracted electric conduction model for concrete.

in the concrete could statistically be described as a resistance R_{CCP}:

$$Z_{CCP} = R_{CCP} \approx \rho_l L\xi/(S\varphi\lambda) \tag{2}$$

where ρ_l is the resistivity of the pore solution in CCP (Ω cm), L the thickness of the concrete in the direction parallel to applied electrical field (cm), S the cross-sectional area of the concrete perpendicular to applied electrical field (cm^2), ξ the tortuosity of CCP, λ the ratio of the volume of the pores forming CCP over the total volume of all the micro-pores in the concrete (%), and φ the porosity of the concrete (% of volume).

Compared with CCP, DCP has more complicated impedance expression because of the "DP." The impedance (Z_{DCP}) of DCP should consist of two parts: the continuous portion (Z_{CP}) of DCP and the discontinuous point (cement paste layers) (Z_{DP}) (Eq. (3)):

$$Z_{DCP} = Z_{CP} + Z_{DP} \tag{3}$$

At the DP point, current has to "penetrate" through the cement paste layer. However, the cement paste has high resistivity and is usually regarded as an "insulator," so a DC current is difficult to "penetrate" through such a cement paste layer. However, the "discontinuous point" can also be treated as a double parallel plate capacitance (C_{DP}) with the cement paste as its dielectric (Fig. 2) whose value can be given by:

$$C_{DP} = (1-\lambda)\varphi S\varepsilon_o\varepsilon_r/d \tag{4}$$

where d is the equivalent cumulative thickness of all the DP points (gel layers or walls) (cm) in the direction paralleled to the electric field, ε_o the vacuum permittivity (8.85×10^{-14} F/cm), and ε_r the relative permittivity of cement paste.

If an AC current is involved in the current conduction, it can pass through the capacitance. In this case, the impedance (Z_{DP}) for the DP point of DCP in the concrete can statistically be written as (Eq. (5)):

$$Z_{DP} = 1/(j\omega C_{DP}) \tag{5}$$

where $j = \sqrt{-1}$ and ω is frequency of AC current passing through the concrete (Hz).

The remaining portion of DCP would have an impedance Z_{CP} similar to that of CCP, which can also be described as a pure resistance:

$$Z_{CP} = R_{CP} = (L-d)\xi\rho_l/[S\varphi(1-\lambda)] \tag{6}$$

Therefore, the total impedance (Z_{DCP}) of DCP in the concrete is equivalent to a resistance R_{CP} plus a capacitance C_{DCP} in series [Eq. (7)]:

$$Z_{DCP} = R_{CP} + 1/(j\omega C_{DP}) = (L-d)\xi\rho_l/[S\ \varphi(1-\lambda)] - jd/[\omega(1-\lambda)S\varphi\varepsilon_o\varepsilon_r] \tag{7}$$

In addition, the "insulator" concrete matrix can be penetrated by an AC current through capacitive charging and discharging effect across the concrete matrix. In this case, the two end faces of the concrete matrix would serve as a double parallel plate capacitance C_{mat}, and the concrete matrix as the dielectric of the capacitance, which can be formulated by:

$$C_{mat} = S\varepsilon_o\varepsilon_r/L \tag{8}$$

and the impedance (Z_{ICP}) of the concrete matrix should be [Eq. (9)]:

$$Z_{ICP} = 1/(j\omega C_{mat}) \tag{9}$$

Strictly speaking, the concrete matrix is not a real insulator to DC current. The hydrated cement (cement gel) in the concrete matrix has limited conductivity, and can be regarded as a resistance R_{mat}. Its contribution to the total conductivity of the concrete is particularly significant when R_{CP} and R_{CCP} become very high under certain circumstances, e.g., the pore solution in the concrete being completely emptied or frozen.

Using corresponding equivalent elements to represent all the above paths and combining them together, an equivalent circuit for the concrete can be obtained as shown in Fig. 4.

Based on Fig. 4, the total impedance (Z) of the concrete would be [Eq. (10)]:

$$Z = 1/\{j\omega C_{mat} + (1/R_{CCP} + 1/R_{mat}) + 1/[R_{CP} + 1/(j\omega C_{DP})]\} \tag{10}$$

Since R_{CCP} and R_{mat} can be incorporated into a single resistance, they cannot be separated in practice. Fortunately,

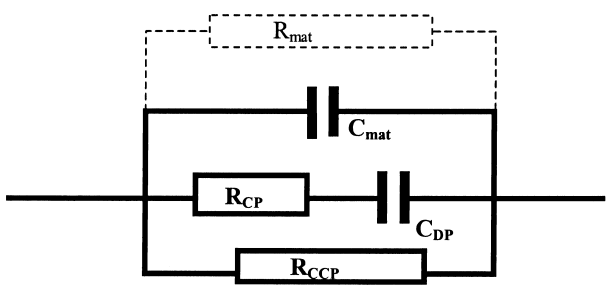

Fig. 4. Detailed equivalent circuit for microstructure of concrete.

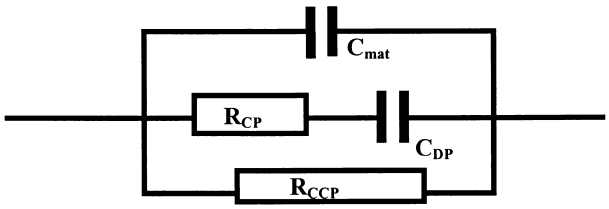

Fig. 5. Equivalent circuit model for concrete.

in most cases, the resistivity of the gel phase in a concrete matrix is so high (i.e., a few orders of magnitude higher than the pore solution) that its conductivity is negligible compared with other conductive paths [Eq. (11)], i.e.,

$$R_{CCP} << R_{mat} \tag{11}$$

Thereby, Eqs. (12) and (13) hold.

$$R_{CCP\|mat} = R_{CCP}R_{mat}/(R_{CCP} + R_{mat}) \approx R_{CCP} \tag{12}$$

$$Z \approx 1/\{j\omega C_{mat} + 1/R_{CCP} + 1/[R_{CP} + 1/(j\omega C_{DP})]\} \tag{13}$$

This means that the R_{mat} path in Fig. 4 can be regarded as an open circuit, and the equivalent circuit (Fig. 4) can be further simplified into an equivalent circuit model as depicted in Fig. 5 for concrete or cementitious system in most cases. In the following discussion, R_{mat} would not be considered if not specified.

The equivalent circuit model (Fig. 5) is much simpler than that proposed by Macphee et al. [22], as only the principle conductive paths are included. Such an equivalent circuit would give out a theoretical EIS spectrum with two capacitive loops as displayed in Fig. 6.

The above equivalent circuit can also be transformed into a conventional circuit (Fig. 7), and the conventional circuit can give out exactly the same EIS spectrum (Fig. 6) as the equivalent circuit model (Fig. 5).

By comparing the conventional circuit (Fig. 7) with the equivalent circuit model (Fig. 5), the following relationships can easily be established:

$$R_0 = R_{CP}R_{CCP}/(R_{CP} + R_{CCP}) \tag{14}$$

$$R_1 = R_{CCP}^2/(R_{CP} + R_{CCP}) \tag{15}$$

$$C_0 = 1/2(1 + R_{CP}/R_{CCP})^2 C_{DP} - [C_{DP}^2 - 4C_{DP}C_{mat}/(1 + R_{CP}/R_{CCP})^2]^{1/2} \tag{16}$$

$$C_1 = 1/2(1 + R_{CP}/R_{CCP})^2 C_{DP} + [C_{DP}^2 - 4C_{DP}C_{mat}/(1 + R_{CP}/R_{CCP})^2]^{1/2} \tag{17}$$

$$R_{CP} = (R_0 + R_1)R_0/R_1 \tag{18}$$

$$R_{CCP} = R_0 + R_1 \tag{19}$$

$$C_{DP} = (C_0 + C_1)[R_1/(R_0 + R_1)]^2 \tag{20}$$

$$C_{mat} = C_0C_1/(C_0 + C_1) \tag{21}$$

where parameters R_0, R_1, C_0, and C_1 can easily be obtained from a measured EIS spectrum using the conventional circuit (Fig. 7), while R_{CP}, R_{CCP}, C_{mat}, and C_{DP} are theoretical parameters with clear physical meanings for concrete microstructure.

The above equations [Eqs. (14)–(21)] also provide an easy method to estimate concrete micro-structural parameters from an experimental EIS spectrum. After R_0, R_1,

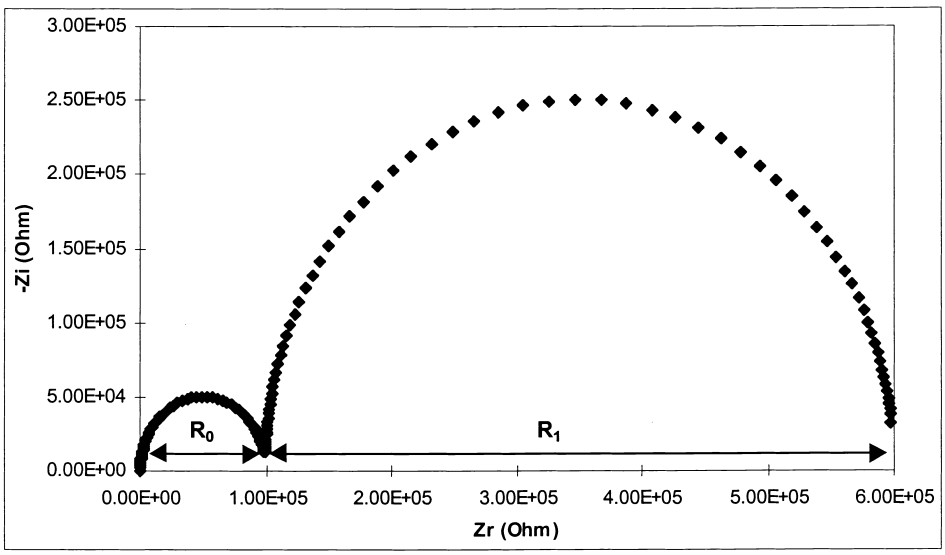

Fig. 6. Theoretical Nyquist EIS spectrum based on the equivalent circuit model as shown in Fig. 5. (the spectrum displayed in this figure is computer-generated using the following parameters: $R_{CP} = 120$ kΩ, $R_{CCP} = 600$ kΩ, $C_{mat} = 6$ pF, and $C_{DP} = 0.9$ nF).

C_0, and C_1 are obtained from the experimental EIS, R_{CP}, R_{CCP}, C_{mat}, and C_{DP} can be calculated by following these equations. In this way, extracting resistance and capacitance values for individual micro-structural features would not be difficult.

Furthermore, with the above equations, the measured parameters, like R_0, R_1, etc, become more meaningful. For example, Eq. (14) suggests that R_0 is actually the overall resistance of all continuously and discontinuously connected micro-pores that are filled with water in a concrete; R_0+R_1 indicates the resistance of the continuously connected micro-pores according to Eq. (19).

3. Theoretical features of equivalent circuit model

The probability for micro-pores to form CCP paths in concrete is relatively low, therefore, $\lambda<<1$. In addition, the cement paste layers that block the continuity of DCP can also be assumed to be much thinner than the apparent concrete thickness ($d<<L$) due to the high porosity of concrete. Therefore, from Eqs. (4) and (8), the following relationship can also easily be deduced [Eq. (22)]:

$$C_{mat} << C_{DP} \tag{22}$$

By substituting it into Eqs. (16) and (17), C_0 and C_1 can be simplified into:

$$C_0 \approx C_{mat} \tag{23}$$

$$C_1 \approx (1 + R_{CP}/R_{CCP})^2 C_{DP} \tag{24}$$

It is obvious that Eq. (25) holds.

$$C_0 << C_1 \tag{25}$$

Eqs. (23) and (24) suggest that, the first capacitive loop in the high-frequency region is mainly associated with the capacitance (C_{mat}) across the concrete matrix. The second capacitive loop in the lower frequency region mainly characterises the capacitance (C_{DP}) of the DPs in the concrete.

The above theoretical features have been demonstrated in some particularly designed experiments, such as the work by Keddam et al. [9].

Keddam et al. [9] obtained three capacitive loops from a cement paste with graphite plates as conducting electrodes on both end faces of the specimen at room RH. They believed that the first loop in the high-frequency region (around 10 MHz) was related to the capacitance and resistance of the cement pastes; while the second capacitive loop in the intermediate frequency range (around 100 kHz) corresponded to the interface of cement paste/graphite electrode; and the third capacitive loop in the low frequency (<100 kHz) should be ascribed to unknown interfacial effect.

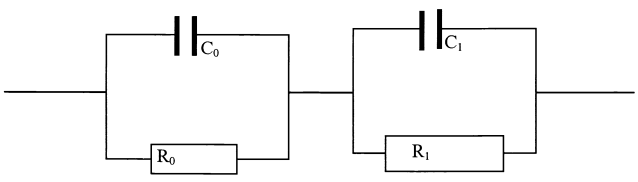

Fig. 7. Conventional circuit of concrete.

Such a postulation is not reasonable for the capacitance of the second loop, because the measured value of the capacitance was of the order of nF/cm^2, which is too small for an interface capacitance. If the interface of the graphite/cement is regarded as a parallel plate capacitance, then the distance between the graphite plates and the cement paste that was in contact with each other should be negligible, say less than 1 μm. In this case, a capacitance much larger than 0.1 μF/cm^2 would be expected, which is about two orders of magnitude higher than the experimental one (some nF/cm^2) [9]. The significant deviation of the experimental value from the theoretically expected result (>0.1 μF/cm^2) suggests the inapplicability of this explanation [9].

If the equivalent circuit model (Fig. 5) proposed in this paper is employed to interpret Kiddam et al.'s results, then the experimental data would be able to fit the theoretical expectations.

As mentioned earlier, the first capacitive loop in the high-frequency region is associated with C_{mat}. If the ε_r of cement paste at room RH is assumed to be 40, then a capacitance of around 4.5 pF/cm^2 (calculated based on the geometric parameters provided in the literature [9]) would be obtained, which is close to the experimental one [9].

The second capacitive loop in the equivalent circuit model (Fig. 5) would mainly be caused by the capacitance (C_{DP}) of the DPs (i.e., the cement paste layers in the DCP). In some senses, the ratio of C_{DP}/C_{mat} is equivalent to the "dielectric amplification factor" [17]. It would be reasonable to assume that $L/d \approx 10^2$ or $d \approx 100$ μm in the case that $L \approx 0.8$ cm [9], then $C_{DP} \approx 0.4$ nF/cm^2 would result, which is also very close to the experimental one [9].

As to the third capacitive loop reported by Kiddam et al. [9], the present author believes that it may have something to do with the oxygen diffusion and reduction reaction at the graphite/cement interface. Such a process usually generates a capacitive loop or Warburg impedance (the slope of $-Z_i$ against Z_r is around 1) in a lower frequency region in the Nyquist diagram, and has a measured capacitance of some μF/cm^2 order of magnitude or even higher.

Most water in the micro-pores of the cement paste, particularly in the relatively large pores like capillary cavities and micro-cracks, would be removed after oven-drying. As it is more likely for large pores to form CCPs, the removal of the water would mainly affect the CCP whose resistance would be dramatically increased after oven-drying. Therefore, the equivalent circuit model (Fig. 5) for the oven-dried cement paste would have an open-circuited R_{CCP} and an extremely high R_{CP}. Corresponding to such a circuit, the Nyquist EIS spectrum should have one capacitive loop alone as described by Kiddam et al. [9].

If insulating polyester sheets were inserted between the graphite plates and cement specimen, the second capacitive loop characterising C_{DP}, would be overwhelmed by the polyester sheet related capacitive features, because the polyester sheets have a thickness of 100 μm, which could form a capacitance with a value close to that of C_{DP}.

Both of the polyester sheets alone and the polyester-sheets-insulated cement specimen have very high impedance, and exhibit very large and non-complete capacitive loops in the Nyquist diagram. A very small relative error in their impedance measurements can cause a very significant absolute difference in the measured impedance, which would lead to an incomplete subtraction of the impedance of the polyester sheet from that of the polyester sheets insulated cement specimen. Consequently, a high remaining impedance could result from such an incomplete subtraction. This might be the reason why the subtracted EIS spectrum still had a large capacitive loop in the low frequency [9]. Moreover, in theory, the large capacitive loop after a complete substation cannot be caused by an electrically (ionic and electronic) blocked boundary on both end faces of the sample as Kiddam et al. [9] suggested, because the blocked boundary effect is actually a capacitance behaviour, which is supposed to be eliminated if a complete subtraction has been conducted.

4. Experimental AC EIS of concrete bulk

Dispersion effect is a very common phenomenon in experimental AC EIS, which makes the capacitance expression more complicated. This issue would not be discussed in this paper.

In most experiments, it is relatively difficult to obtain a complete theoretical EIS spectrum as Fig. 6, due to the accuracy limitation of most electrochemical equipment. Usually, the first high-frequency capacitive loop could be seriously distorted by the equipment and wiring impedance. It could also emerge in the frequency region that is too high and beyond the frequency limit of the equipment. Therefore, in practice, most measured Nyquist EIS spectra usually start from the second capacitive loop, and have only one semicircle, i.e., the second capacitive loop as shown in Fig. 8.

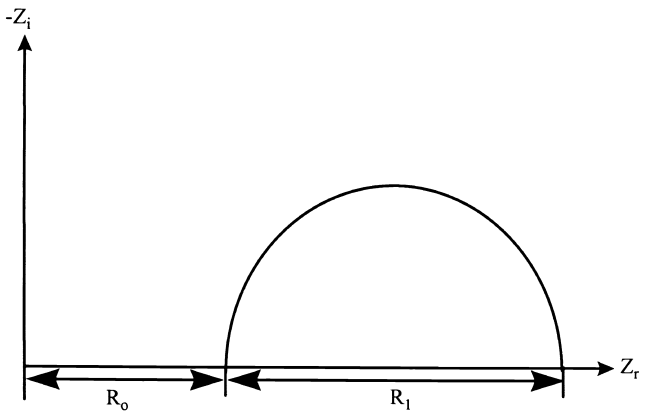

Fig. 8. Experimental AC EIS spectrum for concrete bulk.

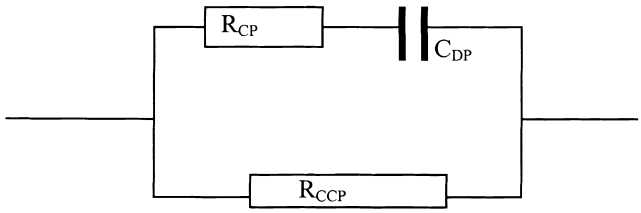

Fig. 9. Simplified equivalent circuit model for concrete bulk.

In this case, the equivalent circuit model can also be further simplified into Fig. 9 under the experimental conditions, because C_{mat} is too small ($C_{mat} \rightarrow 0$), compared with C_{DP}, to be considered within the measurement frequency range. Correspondingly, its conventional equivalent circuit would be simpler too (Fig. 10).

Based on the simplified circuits (Fig. 9 and Fig. 10), the relationships among C_0, C_{mat}, C_1 and C_{DP} can also be simplified into [Eqs. (26)–(28)]:

$$C_0 \approx C_{mat} \approx 0 \tag{26}$$

$$C_1 = (1 + R_{CP}/R_{CCP})^2 C_{DP} \tag{27}$$

$$C_{DP} = C_1[R_1/(R_0 + R_1)]^2 \tag{28}$$

AC EIS has been used to investigate the hydration of cement and the influences of some factors on the hydration process by various researchers [6,7,8,15–18]. The typical features of the EIS spectra can be summarised by the following.

(1) R_1 (Fig. 8) increases dramatically with hydration time. R_0 increases marginally only during the early stage of hydration.

(2) Usually, the capacitive loop with R_1 as its diameter does not appear in an ordinary cement paste until a critical hydration time has been reached. However, in a very low porosity cementitious system, such a delayed appearance of the capacitive loop does not occur.

(3) R_1 of a hydrating cement system containing silica fume is grater than that of a cement without silica fume.

(4) C_1 decreases with hydration time.

(5) Both R_0 and R_1 decrease with a decreasing concrete thickness. If the concrete thickness is too small,

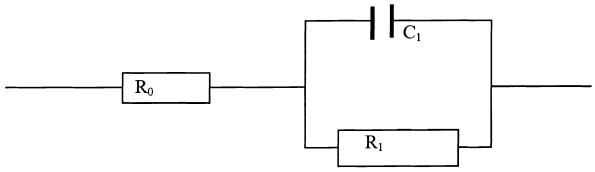

Fig. 10. Conventional equivalent circuit of the simplified model as shown in Fig. 9.

the capacitive loop characterised by R_1 as its diameter could disappear.

(6) R_1 decreases as the water/cement ratio increases.

In order to interpret phenomena (1)–(4) above, an improvement has been made by Xie et al. [8] in their second model, which mainly attributes R_0 to the resistance of the pore solution, rather than to the resistance of unhydrated cement and hydration products as stated in their first model [7]. However, in both models [7,8], R_1 (Fig. 8) was ascribed to an interface resistance (R_f) between the solid (unhydrated cement and hydration products) and liquid (pore solution) phases in the cement paste.

It is well known that, apart from the capacitive effect of charging and discharging processes, current conduction across a solid/solution interface can be carried out in two different mechanisms.

(1) Ions migrate to the interface from the solution, and pass through the interface, then continue to travel in the solid phase. In this case, the solid is usually an ion conductor, otherwise the ions would be accumulated in the vicinity of the interface in the solid side and would finally stop the current conduction.

(2) Ions migrate from the solution to the interface, then Faradic reactions (i.e., electrochemical reactions, or electron exchange between the ions in the solution and species in the solid) occur at the interface, and the charged or discharged species (including electron) continue to travel in the solid. In this case, the interface resistance is termed as transmitting resistance R_t, which is strongly dependent on applied potential or current density.

In a cement paste system, the main ions in the pore solution are OH^-, K^+, Na^+, and Ca^{2+}. At the interface of pore solution/cement gel, if the first mechanism plays the principal role in current conduction, then the cations K^+, Na^+, and Ca^{2+} would be "piled up" in the cement solid, which would dramatically change the properties of the cement solid. Obviously, this is not true. If the second mechanism operates when current flows through the solution/cement interface, then the concrete resistance would change dramatically with applied current or potential. This is rather incorrect. Therefore, the interpretation of R_1 as the interface resistance between the pore solution and cement solid is not convincing.

Phenomena (1)–(6) above can be explained more reasonably using the simplified equivalent circuit model (Fig. 9) proposed in this paper.

(1) Cement hydration is the process by which cement powder turns into C–S–H gel. The latter has much larger volume than the former. Therefore, the expanding cement gel particles during the hydration process would be more likely to block CCP paths and to narrow the DCP paths or to thicken the DP layers. All these changes in CCP and DCP paths would increase R_{CCP} and R_{CP}, resulting in R_1 and R_0 increasing with hydration time. However, the extents of the influence of hydration on R_{CCP} and R_{CP} are different. The hydration can block CCP paths and reduce the number of CCP paths by turning CCP into DCP, whereas it can only narrow the DCP paths or thicken DP layers. Thus, R_{CCP} usually decreases significantly with hydration time. On the other hand, R_{CP} could not be greatly reduced, because some CCP paths after being blocked turn into DP paths that would compensate for the decrease in R_{CP} to some extent. Hence, the overall influence of hydration on R_{CCP} is much more significant than on R_{CP}, i.e., the ratio of R_{CCP}/R_{CP} would increase with hydration time because of $R_{CCP}/R_{CP} = R_1/R_0$ according to Eqs. (18) and (19). This means that R_1 would increase more dramatically with hydration time than R_0.

(2) At the early hydration stage (the first few hours), cement particles are not sufficiently hydrated and their expansion is not significant. All the intervals between cement particles are still filled with water, i.e., the cement paste at this stage is full of CCP paths and had few or no DCP paths. In this case, the simplified model (Fig. 9) can be further simplified into a R_{CCP}, which could not display a capacitive loop in the Nyquist diagram. However, in a very low porosity cement paste, some CCP paths could be quickly blocked by DP and changed into DCP paths, so a capacitive loop would be exhibited very soon after hydration.

(3) The added silica fume, which has much smaller particle size than the Portland cement, stays in the micropores of the cement paste matrix. This could effectively decrease the porosity (φ) of the cement paste. According to Eq. (2), R_{CCP} would increase as φ decreases, which would result in an increasing R_1 [Eq. (15)].

(4) In the equivalent circuit model proposed in this paper, C_{DP} is the double parallel plate capacitance of DP. The hydration would undoubtedly increase the thickness of DP in DCP, which would lower the value of C_{DP}. Consequently, C_1 decreases with the hydration time according to Eq. (27).

(5) When the thickness (L) of the concrete is increased, according to Eqs. (2) and (6), both R_{CCP} and R_{CP} would increase, hence, both R_1 and R_0 increase (Eqs. (14) and (15)). On the other hand, if L decreases, the possibility of the cement paste layers (DP) blocking the continuity of the micro-pores decreases. When L is too small, then the number of the blocked DCP paths becomes extremely low. This is equivalent to a short-circuited R_{CP} in the equivalent circuit model (Fig. 9), therefore, only a single capacitive loop would be displayed in the Nyquist diagram.

(6) Changing the ratio of w/c also alters the porosity of the cement paste. Higher w/c ratio would lead to a higher porosity (φ), thus, R_{CCP} and R_1 would decrease with the increase in w/c ratio according to Eqs. (2) and (15).

5. Conclusions

(1) An equivalent circuit model for concrete has been proposed, which contains meaningful parameters R_{CCP}, R_{CP}, C_{mat}, and C_{DP}. R_{CCP} is the resistance of the continuously

connected micro-pores; R_{CP} is the resistance of the discontinuously connected micro-pores, blocked by cement paste; C_{mat} is the capacitance across the concrete matrix; and C_{DP} is the capacitance of the cement paste blocking the continuity of the connected micro-pores.

(2) According to the proposed model, the parameters demonstrated by the experimental Nyquist EIS have clear meanings. For example, R_0 is the overall resistance of all the micro-pores in the concrete bulk, including continuously and discontinuously connected interstitial gel pores, capillary cavities, and even micro-cracks; R_1+R_0 is the total resistance of the continuously connected micro-pores in concrete.

(3) From the measured parameters R_0, R_1, C_0, and C_1, the meaningful parameters R_{CCP}, R_{CP}, C_{DP}, and C_{mat} can be easily calculated.

(4) The proposed model can successfully explain the experimental phenomena observed by other researchers, such as the influences of hydration time, silica fume, and water/cement ratio on the capacitive loops in high-frequency range, etc.

Acknowledgments

The author would like to express his sincere gratitude to Ms. Ying Yu for her encouragement, support, and assistance. Dr. Ahmad Shayan is also gratefully acknowledged for his beneficial advice and discussions in preparing this manuscript.

References

[1] W.J. McCarter, S. Garvin, N. Bouzid, Impedance measurements on cement paste, J Mater Sci Lett 7 (1988) 1056–1057.
[2] C.A. Scuderi, T.O. Mason, H.M. Jennings, Impedance spectra of hydrating cement pastes, J Mater Sci 26 (1991) 349–353.
[3] K. Brantervik, G.A. Niklasson, Circuit models for cement based materials obtained form impedance spectroscopy, Cem Concr Res 21 (1991) 496–508.
[4] W.J. McCarter, R. Brousseau, The AC response of hardened cement paste, Cem Concr Res 20 (1990) 891–900.
[5] P. Gu, Z. Xu, J.J. Beaudoin, Application of AC impedance techniques in studies of porous cementitious materials: I. Influence of solid phase and pore solution on high frequency resistance, Cem Concr Res 23 (1993) 531–540.
[6] P. Gu, P. Xie, J.J. Beaudoin, R. Brousseau, AC impedance spectroscopy: II. Microstructural characterization of hydrating cement-silica fume systems, Cem Concr Res 23 (1993) 157–168.
[7] P. Gu, P. Xie, J.J. Beaudoin, B.R. Brousseau, AC impedance spectroscopy: I. A new equivalent circuit model for hydrated portland cement paste, Cem Concr Res 22 (1992) 833–840.
[8] P. Xie, P. Gu, Z. Xu, J.J. Beaudoin, A rationalized AC impedance model for microstructural characterization of hydrating cement systems, Cem Concr Res 23 (1993) 359–367.
[9] M. Keddam, H. Takenouti, X.R. Novoa, C. Andrade, C. Alonso, Impedance measurements on cement paste, Cem Concr Res 27 (1997) 1191–1201.
[10] Z. Xu, P. Gu, P. Xie, J.J. Beaudoin, Application of AC impedance techniques in studies of porous cementitious materials: II. Relationship between ACIS behavior and the porous microstructure, Cem Concr Res 23 (1993) 853–862.
[11] M.F. Monenor, A.M.P. Simoes, M.M. Salta, M.G.S. Ferreira, The assessment of the electrochemical behavior of fly ash-containing concrete by impedance spectroscopy, Corr Sci 35 (1993) 1571–1578.
[12] G.A. Niklasson, A. Berg, L. Brantervik, Dielectric properties of porous cement mortar: fractal surface effect, J Appl Phys 79 (1991) 93–96.
[13] P. Gu, P. Xie, Y. Fu, J.J. Beaudoin, AC impedance phenomena in hydrating cement systems: frequency dispersion angle and pore size distribution, Cem Concr Res 24 (1994) 86–88.
[14] P. Lay, P.F. Lawrence, N.J. Wilkins, D.E. Williams, An AC impedance study of steel in concrete, J Appl Electrochem 15 (1985) 755–766.
[15] Z. Xu, P. Gu, P. Xie, J.J. Beaudoin, Application of AC impedance techniques in studies of porous cementitious materials: III. ACIS behavior of very low porosity cementitious systems, Cem Concr Res 23 (1993) 1007–1015.
[16] P. Xie, P. Gu, Y. Fu, J.J. Beaudoin, AC impedance phenomena in hydrating cement systems: detectability of the high frequency ARC, Cem Concr Res 24 (1994) 92–94.
[17] B.J. Christensen, R.T. Coverdale, R.A. Olson, S.J. Ford, E.J. Garboczi, H.M. Jennings, T.O. Mason, Impedance spectroscopy of hydrating cement-based materials: measurement, interpretation, and application, J Am Ceram Soc 77 (1994) 2789–2804.
[18] B.J. Christensen, T.O. Mason, H.M. Jennings, Influence of silica fume on the early hydration of portland cements using impedance spectroscopy, J Am Ceram Soc 75 (1992) 939–945.
[19] H.W. Whittington, J. McCater, M.C. Forde, The conduction of electricity through concrete, Mag Concr Res 33 (1981) 48–60.
[20] W.J. McCarter, S. Garvin, Dependence of electrical impedance of cement-based materials on their moisture condition, J Phys D: Appl Phys 22 (1989) 1773–1776.
[21] W.J. McCarter, H. Ezirim, AC impedance profiling within cover zone concrete: influence of water and ionic ingress, Adv Cem Res 10 (1998) 57–66.
[22] D.E. Macphee, D.C. Sinclair, S.L. Stubbs, Electrical characterization of pore reduced cement by impedance spectroscopy, J Mater Sci Lett 15 (1996) 1566–1568.
[23] D.E. Macphee, D.R. Sinclair, S.L. Cormack, Development of an equivalent ceircuit model for cement pastes from microstructural considerations, J Am Ceram Soc 80 (1997) 2876–2884.
[24] S.L. Cormack, D.E. Macphee, D.R. Sinclair, An AC impedance spectroscopy study of hydrated cement pastes, Adv Cem Res 10 (1998) 151–159.
[25] S.J. Ford, J.H. Hwang, J.D. Shane, R.A. Olson, G.M. Moss, H.M. Jennings, T.O. Mason, Dielectric amplification in cement pastes, Adv Cem Based Mat 5 (1997) 41–48.